
Influence of Probe Pressure on Human Skin Diffuse Reflectance Spectroscopy Measurements¹

J. A. Delgado Atencio^{a,c}, E. E. Orozco Guillén^{b,c}, S. Vázquez y Montiel^c,
M. Cunill Rodríguez^{a,c}, J. Castro Ramos^c, J. L. Gutiérrez^d, and F. Martínez^d

^a Departamento de Física, Centro de Aplicaciones Tecnológicas y Desarrollo Nuclear (CEADEN), Cuba

^b Departamento de Física, Universidad de Carabobo, Facultad Experimental de Ciencia y Tecnología, Venezuela

^c Departamento de Óptica, Instituto Nacional de Astrofísica Óptica y Electrónica (INAOE), México

^d Departamento de Oncología, Hospital de la Benemérita Universidad Autónoma de Puebla, México

Received January 19, 2009; in final form, January 19, 2009

Abstract—In a routine procedure for collecting human skin spectra using fiber optic diffuse reflectance spectroscopy, the fiber optic probe is put gently in contact with the skin surface. The purpose of this work is to investigate the influence of probe pressure on *in-vivo* diffuse reflectance spectroscopy measurements performed by a non-trained operator. In addition, we include simulation using diffusion theory that explains the behavior of diffuse reflectance spectra with the increase of probe pressure.

Key words: diffuse reflectance spectroscopy, tissue optics, diffusion theory.

DOI: 10.3103/S1060992X09010020

INTRODUCTION

Diffuse reflectance spectroscopy is a well established optical tool to investigate the metabolic state and the structure of human skin and other tissues [1–3]. Two experimental approaches are commonly used to record the human skin spectrum *in vivo*: the first is based on the use of an integrating sphere that collects the total diffuse reflectance from the skin measurement site and the second one consist of a fiber optic probe that captures only a fraction of this reemitted light [4]. The second approach is preferred for applications in a clinical environment because of its flexibility. In a routine procedure for collecting skin spectra, the fiber optic probe is put gently in contact with the skin surface. Therefore, a pressure is created that might affect the profile of the diffuse reflectance spectrum. To the best of our knowledge, pressure effects on *in vivo* diffuse reflectance spectroscopy of human skin have been reported by few researchers [5–7]. For instance, Randeberg [5] reported the typical effect of applying strong pressure onto the collecting sphere during the measurement of diffuse reflectance in the spectral region (400–850 nm) in a volunteer. This author reported that at a strong pressure the intensity of the spectrum is increased at wavelengths higher than 600 nm while is decreased below this wavelength in comparison with the spectra corresponding to non-pressure against the skin. In an *in vivo* discrimination study of early melanoma, Murphy et al. [6] reported that varying probe pressure did affect the spectra measured from a small area of normal skin resulting in a variability less than 5% and that a trained operator was able to achieve repeatability on the order of 2%. Recently Chen et al. [7] have performed NIR (1100–1700 nm) diffuse reflectance spectroscopy *in vivo* in ten volunteers. The spectra were taken from skim palm and the results show that diffuse reflectance decreases with increasing contact pressure under the contact state. The purpose of this work is to investigate the influence of probe pressure on human skin diffuse reflectance spectra in the range of 345–1000 nm when the measurements are performed by a single non-trained operator.

MATERIALS AND METHODS

Experimental Set-Up

The experimental set-up for diffuse reflectance spectra measurements consist of a commercial optical fiber spectrometer from Ocean Optic inc. (USB4000), a tungsten halogen light source (HL-2000), and bifurcated fiber optic probe (R600-7-VIS/125F). The common end of the fiber-optic probe has a central collec-

¹ The article is published in the original.

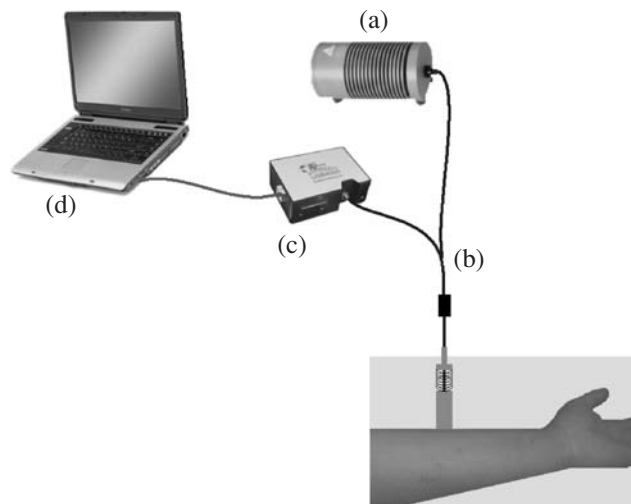


Fig. 1. Schematic of the experimental set-up employed to collect clinical diffuse reflectance spectra of human skin: (a) light source, (b) bifurcated fiber optic probe, (c) optical fiber spectrometer and (d) laptop computer.

tion fiber surrounded by six concentric illumination fibers (600 μm diameter and a numerical aperture of 0.22) yielding an hexagonally compact array enclosed in a stainless steel tube with a 3.1 mm outer diameter. The measurement range of the system is 345–1037 nm with a spectral resolution of 2 nm. Spectra were collected and saved using the Spectrasuite software stored in a laptop computer connected to the USB4000 spectrometer via the USB port. Spectra were calibrated against a diffuse reflectance standard of Teflon. A schematic of the experimental set-up is provided in Fig. 1.

The original probe above described was lightly modified at its common tip by incorporating a metallic cylindrical accessory with a glass window (170 μm of thick and 8.20 mm of diameter) at one of its tips in order to protect the fibers from contamination and deterioration during their use in this application. The metallic accessory has an external diameter of 8.25 mm and a length of 50 mm. Following Nath et al. [8] paper, a spring loaded attachment was coupled to the previously modified probe to guarantee calibrated levels of pressure on the skin measurement site. In Fig. 2 a picture of the original and modified fiber optic probe is presented. The attachment b1 consists of a scaled metallic sleeve, a spring and a moving part M used to comprise the spring.

In Vivo Human Skin Spectra

The subjects participating in this study were patients attending to the service of oncology of the hospital of the Benemérita Universidad Autónoma de Puebla, México that were invited to be part of this research. We have studied 45 volunteers for a total 45 diffuse reflectance spectra recorded in normal sites and 1 at a skin lesion. All the volunteers were adults with age in a range between 20 and 76 years. Our group of study include 28 females and 17 males individuals of dark, light dark, and light skin, respectively.

The inner forearm of volunteers was selected as the measurement site for this in vivo study. Volunteers rested their forearm on a $45 \times 28 \text{ cm}^2$ metallic plate while the operator oriented the surface of the measurement site horizontally. The levels of applied pressure were denoted as P0, P1, P2, P3, P4, P5 corresponding to 0, 0.202, 0.388, 0.576, 0.787 and 0.933 N/cm^2 , respectively. Once the probe tip was contacting the measuring site (the operator visually monitored that the flat surface of the probe was in a gentle contact with the skin by looking tangentially to both surfaces) the moving part of the spring loaded pressure attachment was set at the zero level of the lineal scale on the sleeve. Then the moving part was displaced consecutively over the linear scale to each of the five positions on the lineal scale of the probe corresponding to increasing values of the probe contact pressure. The increment between steps was of 2 mm in the linear scale. Only one diffuse reflectance spectrum was collected at each pressure level, being the average time at each level around 5 s.

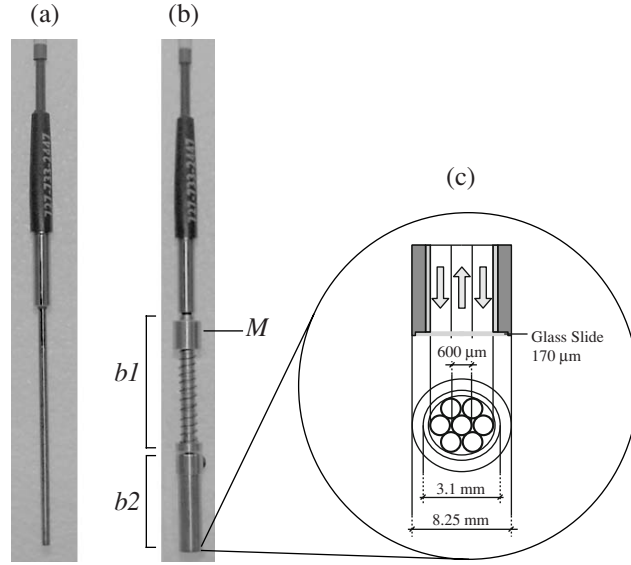


Fig. 2. Fiber optic probe details: (a) original and (b) modified fiber probe showing the attachments b1 and b2 for controlling the pressure on the skin surface and protecting original fibers from damages and contamination, respectively. In (c) side and front view of the source-detector geometry at the probe tip.

Simulation of Diffuse Reflectance Spectra

Radial reflectance model. Diffuse reflectance spectra collected with the fiber probe were simulated using the diffusion theory model for radial resolved reflectance $R(\rho)$ developed by Farrell et al. [9]. In this model the light source is a pencil beam normally incident from a medium of refractive index n_a onto the surface of an homogeneous semi-infinite tissue of refractive index n_t and optical parameters μ_a and μ'_s . Specifically we use the single scatter site model in which all the interactions of the original pencil beam occurs at a single interaction site placed at a depth Z_0 equal to one transport mean free path ($1/(\mu_a + \mu'_s)$). The fluence rate $\Phi(\rho)$ is zero at an extrapolated boundary (EB) placed at $Z = -Z_b = -2AD$ where $D = 1/3(\mu_a + \mu'_s)$ and A is parameter related to the uniformly diffuse radiation at the interface air-tissue. The parameter A is a function of the relative refractive index $n_r = n_t/n_a$ of tissue and surrounding medium. In order to satisfy the above mentioned EB condition a virtual negative point source is placed at $Z = -(Z_0 + 2Z_b)$ resulting the equation 1 corresponding to the analytical expression for the radial resolved reflectance $R(\rho)$ which depends only of three optical parameters (μ_a, μ'_s, n_r):

$$R(\rho) = \frac{a'}{4\pi} \left[\left(\frac{1}{\mu'_t} \right) \left(\mu_{\text{eff}} + \frac{1}{r_1} \right) \frac{\exp(-\mu_{\text{eff}} r_1)}{r_1^2} + \left(\frac{1}{\mu'_t} + 2Z_b \right) \left(\mu_{\text{eff}} + \frac{1}{r_2} \right) \frac{\exp(-\mu_{\text{eff}} r_2)}{r_2^2} \right] \quad (1)$$

with $r_1 = \sqrt{(Z_0)^2 + \rho^2}$, $r_2 = \sqrt{(Z_1)^2 + \rho^2}$ where $Z_0 = \frac{1}{\mu'_t}$ and $Z_1 = -(Z_0 + 2Z_b)$ $\mu'_t = \mu_a + \mu'_s$ is the total interaction coefficient, $\mu_{\text{eff}} = \sqrt{3\mu_a(\mu_a + \mu'_s)}$ is the effective attenuation coefficient and $a' = \mu'_s/(\mu_a + \mu'_s)$ is the transport albedo.

Figure 3 shows the parameters of the model and the geometrical localization of the elements and parameters involved in the above described model. The simulation for the fiber optic probe of our experimental set-up (a central collection fiber surrounded by six concentric illumination fibers all fibers of 600 μm diameter and a numerical aperture of 0.22) was treated as a fundamental “two fiber system” at a constant source-detector distance ($\rho = 720 \mu\text{m}$) place in contact with tissue surface ($Z = 0$).

Skin model. We assume a simple model of skin consisting of two layers, namely epidermis with a finite size L and dermis as a semi-infinite medium. Epidermis is considered, in a first approach, as an absorbing medium where the main absorber is melanin. Dermis is considered as an absorbing and scattering medium where blood (oxy hemoglobin and deoxy hemoglobin) and water are the main absorbers while collagen

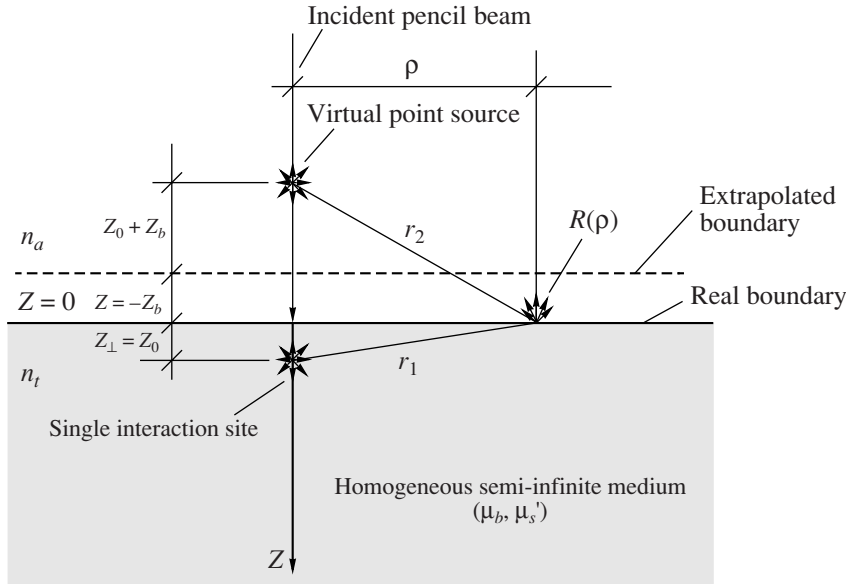


Fig. 3. Schematic situation illustrating all the parameters and the geometrical relationships involved in the diffusion model derived by Farrell et al. for the radial resolved reflectance $R(\rho)$ in a semi-infinite medium of optical parameter (μ_a, μ_s', n_t) surrounded by a medium of refractive index n_r .

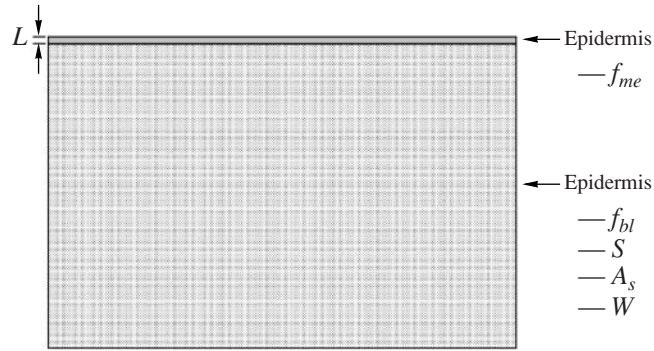


Fig. 4. Simple two medium model selected for skin geometry. The first medium is a thin homogeneous layer of thickness L where the main absorber is melanin which is homogeneously distributed in the volume of this layer. The second medium is a semi-infinite space where main absorbers are blood and water, and the main scattering centers are collagen fibers. Both, scattering and absorber centers are homogeneously distributed in this second medium.

fibers are the principal scattering centres. A picture of the skin model is shown in Fig. 4 indicating the principal biological parameters of the model in each layer.

The epidermis absorption coefficient $\mu_{aE}(\lambda)$ was taken from Jacques [10]:

$$\mu_{aE}(\lambda) = f_{me}\mu_{a_me}(\lambda) + (1 - f_{me})\mu_{a_base}(\lambda), \quad (2)$$

where f_{me} is the volume fraction of melanosomes in epidermis. The absorption coefficient of the interior of melanosomes is approximated as

$$\mu_{a_me}(\lambda) = 6.6 \times 10^{11} \lambda^{-3.33}. \quad (3)$$

The baseline absorption coefficient $\mu_{a_base}(\lambda)$ of epidermis and dermis is the same and is approximated as

$$\mu_{a_base}(\lambda) = 0.244 + 83.5 \exp((\lambda - 154)/66.6). \quad (4)$$

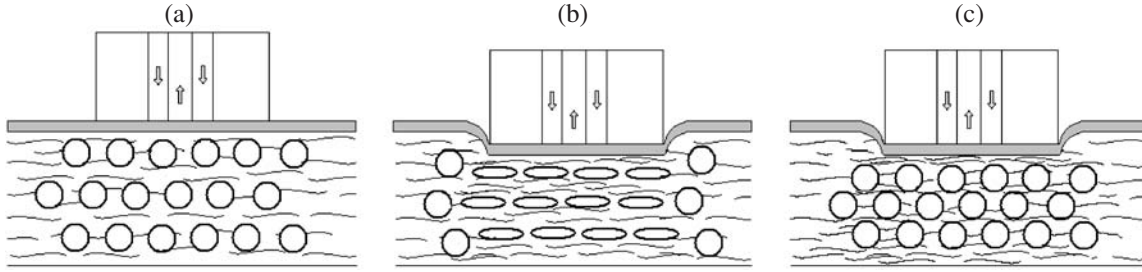


Fig. 5. Effect of probe pressure on blood vessels (circles in normal state or ellipses under pressure effect) and collage fibers (curves) for the two simulated situation performed in this study. (a) Normal state of blood vessel and collagen fibers, (b) blood volume fraction f_{bl} and parameter A_s are both affected by the increasing values of probe pressure on skin. (c) only the parameter A_s of scattering is affected during the compression of skin while blood vessel are assumed to be constant in its dimensions and shape.

Dermis absorption coefficient $\mu_{aD}(\lambda)$ was taken from Jacques¹⁰ and its expression includes the blood volume fraction f_{bl} and the water content W as a parameters:

$$\mu_{aD}(\lambda) = f_{bl}\mu_{a_blood}(\lambda) + (1 - f_{bl})\mu_{a_base}(\lambda) + W\mu_{a_water}(\lambda) \quad (5)$$

in this expression $\mu_{a_blood}(\lambda)$ and $\mu_{a_water}(\lambda)$ are the absorption coefficients of blood and water, respectively. The absorption coefficient of blood is given by the expression:

$$\mu_{a_blood}(\lambda) = S\mu_{a_oxy}(\lambda) + (1 - S)\mu_{a_deoxy}(\lambda), \quad (6)$$

here S represents oxygen saturation and is another parameter of the simulation and $\mu_{a_oxy}(\lambda)$ and $\mu_{a_deoxy}(\lambda)$ are the absorption coefficient of the oxygenated and deoxygenated hemoglobin molecule, respectively.

Dermis scattering coefficient was taken from Jacques¹²

$$\mu'_{sD}(\lambda) = A_s\mu'_{sREF}(\lambda), \quad (7)$$

where $\mu'_{sREF}(\lambda) = \mu'_{sRayleigh}(\lambda) + \mu'_{sMie}(\lambda) = 1.74 \times 10^{12}\lambda^{-4} + 4.59 \times 10^3\lambda^{-0.913}$ is a reference skin scattering spectrum obtained from *ex vivo* measurements which is scaled by means of the parameter A_s to adjust to scattering spectrum found in *in vivo* measurements. This parameter accounts for slight variations of scattering coefficient between individuals or body sites.

We assume that skin is a soft tissue and hence we might conclude that pressure levels applied on the fiber probe area (diameter of 8.25 mm) are likely to locally increase the total number of scattering particles per unit volume of skin with the corresponding increase of the scattering coefficient. We assume that probe pressure primary affect dermal collagen fibers while its effect on other scattering centers is negligible. We assume that for a given skin site the reduced scattering coefficient is incremented via the parameter A_s . In a first approach we considered a linear relationship between the parameter A_s and probe pressure P .

The compression of skin layers can also produce a constriction of blood vessels which might reduce both volume fraction of blood and oxygen level. The oxygen level is take into account by means of the oxygen saturation S . Here is also assumed a decreasing linear behavior between the parameter f_{bl} and probe pressure P .

A combination of the above described models (radial reflectance and two skin model) and the basic assumptions considered were used to simulate the influence of probe pressure on the diffuse reflectance spectra measurements performed with our fiber optic spectrometer. Simulation of the spectra that includes the model described is performed using Matlab©. We focused on two different situations that might be occurring during the experimental measurements of diffuse reflectance spectra when a set of five probe pressure levels was continuously exerted on the skin surface. These situations are described as follows.

In the *first situation* we assumed that during the increase of probe pressure the blood volume fraction f_{bl} decreases and the scattering amplitude A_s , corresponding to the reduced scattering coefficient of generic skin¹², increases. The series of values for these parameters were chosen as: 3, 2.4, 1.8, 1.2,

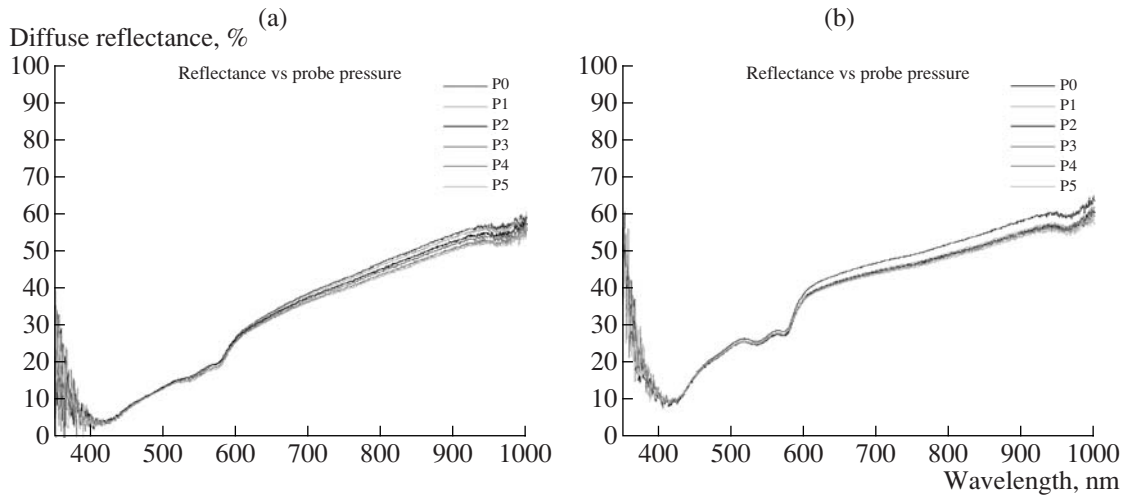


Fig. 6. Typical diffuse reflectance spectra over the entire instrument spectrum from 345–1037 nm as function of the applied pressure onto the skin. (a) Dark skin female volunteer of 22 year, (b) light skin male volunteer of 25 year.

0.6, 0.3% and 3.0, 3.5, 4.0, 4.5, 5, 5.5 for f_{bl} and A_s , respectively. Oxygen saturation S , melanin volume fraction f_{me} , epidermis thickness L and water content W were held constant at 90%, 25%, 70 μm and 90%, respectively.

In the *second situation* we assumed that during the increase of probe pressure the blood volume fraction f_{bl} remains constant at 1% while the scattering amplitude A_s is increased taking the values 3.0, 3.5, 4.0, 4.5, 5, 5.5.

In Fig. 5 is presented a picture of the local effect of probe pressure on blood vessels and collagen fibers for both situations above described at a given level of probe pressure exerted on skin.

RESULTS

Typical diffuse reflectance spectra recorded using five different pressures levels against the skin are shown in Fig. 6. Spectra display characteristic minima around 540 and 578 nm exhibiting the so-called “W” pattern which has his origin in the absorption spectrum of oxy-hemoglobin molecule. The “W” pattern in the diffuse reflectance spectra is more pronounced in light skin volunteers (Fig. 6b) than in dark skin ones (Fig. 6a) at all the probe pressures applied. Even when signal noise ratio of the measurement system is not good enough at shorter wavelengths, a minimum around 420 nm due to oxyhemoglobin absorption spectra (Soret band) can be observed. There is not remarkable difference in diffuse reflectance spectra at different pressures in this spectral band. On the contrary, as shown in Fig. 6, at wavelengths above 600 nm the intensity of diffuse reflectance spectra decreases with increasing probe pressure. This behavior was observed in 38 out of 46 measured spectra in this study. Finally, it is important to notice that in Fig. 6a the P0 spectrum, corresponding to zero probe pressure onto the skin, is relatively more separated from the series of spectra P1–P5 than in Fig. 6b.

Figure 7 shows the two primary patterns of diffuse reflectance observed in the spectral region of 530–680 nm when probe pressure was increased (P0–P5) onto the measurement site. Figure 7a shows the first pattern, which we denote from now on as “pivot pattern,” and Figure 7b presents the second pattern, denoted as “parallel pattern.” In Fig. 7a is clearly observed that diffuse reflectance spectra recorded at different probe pressure have a pivot point around the wavelength of 590 nm. This behavior was found in 7 out of 46 measured spectra with the pivot wavelength λ_{piv} ranging in a relative narrow spectral region (590–615 nm). Above λ_{piv} diffuse reflectance intensity decreases when probe pressure is increased while below λ_{piv} diffuse reflectance increases as the probe pressure is increased.

Figure 7b displays that diffuse reflectance spectra is uniformly decreased in the wavelength region 530–680 nm when the probe contact pressure is increased. This behavior of diffuse reflectance spectra was found in 4 out of 46 measured spectra. Therefore no pivot wavelengths exist in this case. The remaining 35 spectra

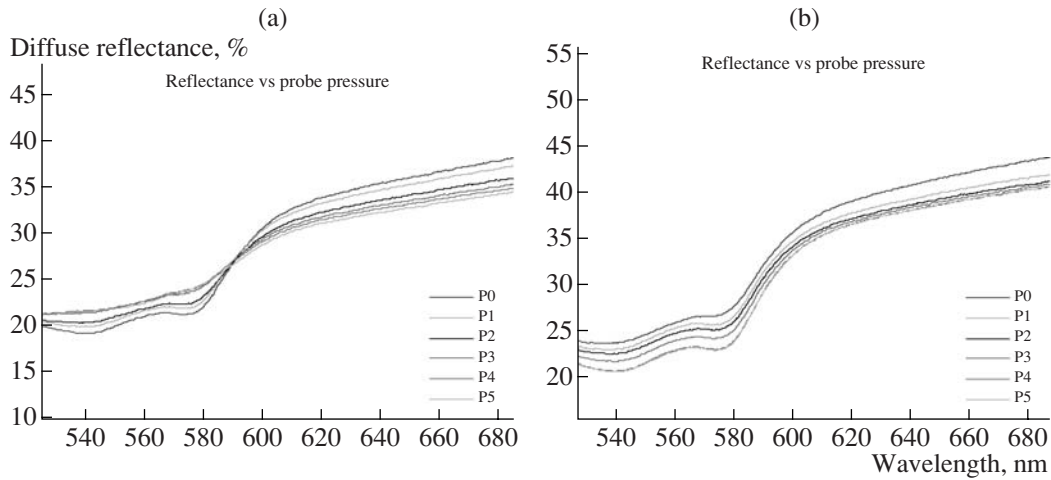


Fig. 7. Two primary patterns of diffuse reflectance spectra found in the 530–680 nm region when probe pressure is increased. (a) Pivot pattern, (b) parallel pattern.

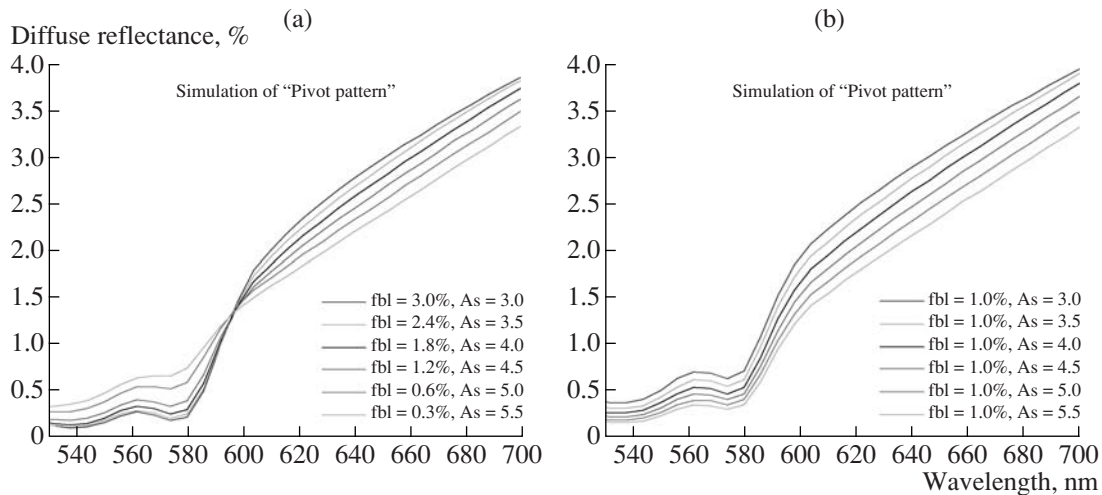


Fig. 8. Simulation of diffuse reflectance spectra of human skin at different probe pressures. (a) Blood volume fraction and scaling scattering factor are varied simultaneously, (b) blood volume fraction fbl was held constant at 1% while scattering amplitude was increased.

were either totally different from the herein called “pivot or parallel patterns” or exhibited some grade of similarity with one of them.

Results of simulation are shown in Figs. 8a and 8b which qualitative explain the results presented previously in Figs. 7a and 7b, respectively. We analyze in details these results in next section.

DISCUSSION

As shown in the result section, at wavelengths above 600 nm the intensity of diffuse reflectance spectra decreases with increasing probe pressure. Our results regarding this topic are not in agreement with the results reported by Randeberg⁵ using an Ocean Optic ISP-REF integrating sphere probe in contact with skin. The author reported that diffuse reflectance intensity increases when a strong pressure was applied. We suppose that some explanation to this opposite results (if not typographical mistake is present in the legend of figure) might be found taking into account the difference between the illumination and collection geometry of both experiments.

We attribute the difference between Fig. 6a and Fig. 6b, concerning the proximity of P0 spectrum to the series of spectra P1–P5, to the variability in the procedure of application of the initial zero pressure P0 by the operator. This variability arises from an still unperfected system of probe pressure control: the initial measurement at P0 is affected in certain extent by the application of a variable fraction of probe weight.

Coefficients of variation (CV) are employed as relative measures of variation. The CV is defined as the standard deviation expressed as a percentage of the mean and is affected by the value of the mean, as well as by the size of the standard deviation. In this work, the variability of the measures, caused by the effects of the pressure applied on the skin, in the case of the pivot pattern it is 4.82% while for the parallel pattern was 3.91%. This variability is inferior to the 5%, as he was reported by Murphy et al.

Regarding the simulations, it is important to note that diffusion approximation breaks down at short source detector distances. Even though some authors has used it to extract optical properties of human tissues from measured diffuse reflectance spectra for probe geometries similar to the one we used in our experiment. Based on these results and verifications of the validity of this approach is that we carried out our simulations specially starting with Farrel et al. formulation. The experimental results of Fig. 7 are qualitatively explain using diffusion approximation and the optical model used when a series of relatively high values of the scattering scaling factor A_s is assumed as representative of human skin for both simulated situations. Simultaneously a series of relatively high values of blood volume fraction is assumed to obtain the pivot pattern. Changing a series of scaling factor, for the blood volume fraction in the series used, is possible to obtain different position for the pivot point in the plane (R, λ) following the general trend that the higher the scaling factor the higher the λ_{piv} found for curve of Fig. 8a. We consider that the simulations presented could be substantially improved using Monte Carlo simulations for a two fibers geometry in a first approach and more accurate results in a more realistic simulation including the deformation of skin surface with the increasing probe pressure. It is worthwhile to mention that we considered that the dynamic process taking place during pressure application on the skin occurs without a total depletion of oxygen sources which in some cases might be explained by an incomplete occlusion of blood vessel or a short total measurement time of diffuse reflectance spectra.

CONCLUSIONS

The findings of this research contribute to elucidate the influence of probe pressure on diffuse reflectance spectroscopy measurements: to our knowledge there is not a paper reporting and explaining the behavior of “pivot” and “parallel” patterns presented in this work. However, in our opinion this issue should be subjected to further studies that include a better control of applied probe pressure by the operator during clinical conditions and a the development of others model that take into account a more realistic dependence between optical parameters and the pressure of fiber probe onto the skin. These preliminary results might be used also to investigate the vascular dynamic processes from measurements of diffuse reflectance spectra.

ACKNOWLEDGMENTS

We acknowledge to CONACYT for supporting the BIOMEDICAL OPTICS program at INAOE, Mexico and to the authorities of the Hospital of the Benemérita Universidad Autónoma de Puebla, México for its support in this study.

REFERENCES

1. Belenkaia, L., *Electronic Laboratory Note Book Assisting Reflectance Spectrometry in Legal Medicine*, http://arxiv.org/PS_cache/cs/pdf/0612/0612123v1.pdf Accessed December 2006 accessed January 25, 2006.
2. Jacques, S.L., Saidu, I., Ladner, A., and Oelberg, D., Developing an Optical Fiber Reflectance Spectrometer to Monitor Bilirubinemia in Neonates, in *Laser Tissue Interaction-1996*, Jacques, S.L., Ed., *Proc. SPIE*, vol. 2975, San José, CA, 1997, pp. 115–124.
3. Bigio, I.J. and Bown, S.G., Spectroscopic Sensing of Cancer and Cancer Therapy, *Cancer Biology and Therapy*, 2004, vol. 3, no. 3, pp. 259–267.
4. Norvan, L.T., Fiskerstrand, E.J., Köning, K., et al., *Proc. SPIE*, 2002, vol. 2624, pp. 155–164.
5. Randeberg, L.L., *Diagnostic Applications of Diffuse Reflectance Spectroscopy*, Doctoral Thesis, Norwegian University of Science and Technology, Trondheim, Norway, 2005.
6. Murphy, B.W., Webster, R.J., Turlach, B.A., et al., Toward the Discrimination of Early Melanoma from Common and Dysplastic Nevus Using Fiber Optic Diffuse Reflectance Spectroscopy, *Journal of Biomedical Optics*, 2005, vol. 10, no. 6, p. 064020, 1–9.

7. Chen, W., Liu, R., Xu, K., and Wang, R.K., Influence of Contact State on NIR Diffuse Reflectance Spectroscopy in vivo, *Journal of Physics D: Applied Physics*, 2005, vol. 38, pp. 2691–2695.
8. Nath, A., Rivoire, K., Chang, S., et al., Effect of Probe Pressure on Cervical Fluorescence Spectroscopy Measurements, *Journal of Biomedical Optics*, 2004, vol. 9, no. 3, pp. 523–533.
9. Farrel, T.J., Patterson, M.S., and Wilson, B., A Diffusion Theory Model of Spatially Resolved, Steady-State Diffuse Reflectance for the Noninvasive Determination of Tissue Optical Properties in vivo, *Med. Phys.*, 1992, vol. 19, pp. 879–888.
10. Jacques, S.L., Skin Optics, 1998, <http://omlc.ogi.edu/news/jan98/skinoptics.html>, accessed January 5, 2006.
11. Prahl, S.A., Optical Absorption of Hemoglobin, <http://omlc.ogi.edu/spectra/hemoglobin/index.html>, accessed January 25, 2006.
12. Jacques, S.L., Spectroscopy Determination of Tissue Optical Properties Using Optical Fiber Spectrometer, *Special Lecture presented at SPIE Photonics West*, 2005.